

Euhedral awaruite in the Allende meteorite: Implications for the origin of awaruite- and magnetite-bearing nodules in CV3 chondrites

ALAN E. RUBIN

Institute of Geophysics and Planetary Physics, University of California, Los Angeles, California 90024, U.S.A.

ABSTRACT

A large ($290 \times 510 \mu\text{m}$) opaque nodule (nodule 1) enclosed in a low-FeO porphyritic olivine chondrule in the Allende CV3 carbonaceous chondrite is comprised of 9 vol% euhedral awaruite, 85 vol% magnetite, 5 vol% pentlandite, and 1 vol% merrillite. The awaruite grains are zoned in Co: centers contain ~15% more Co than edges. The major phases in nodule 1 differ in composition from the corresponding phases in other opaque nodules: awaruite is richer in Ni (71 vs. 65–67 wt%), magnetite is poorer in Al_2O_3 (<0.04 vs. 0.45–0.74 wt%), and pentlandite is richer in Ni (28.4 vs. 19–21 wt%) and Co (2.5 vs. 0.76–0.92 wt%).

The similarity in mineralogy between nodule 1 and other opaque nodules suggests that all formed by the same general sequential process: (1) nebular oxidation of kamacite in chondrule precursors, (2) chondrule formation, (3) development of immiscible magnetite-rich melt droplets within the molten chondrule, (4) crystallization of taenite and magnetite (plus or minus sulfide and phosphate) to form opaque nodules, and (5) transformation of taenite into awaruite \pm tetrataenite at temperatures of $\leq 500^\circ\text{C}$. Taenite was the sole liquidus phase in nodule 1 and thus developed euhedral morphologies upon crystallization; in the other nodules, taenite crystallized along with or subsequent to magnetite and did not form euhedral grains.

INTRODUCTION

Awaruite (ideally Ni_3Fe) is a face-centered cubic (fcc) mineral with an ordered superlattice: Fe atoms are situated at cube corners and Ni atoms at face centers (Leech and Sykes, 1939; Nickel, 1959). According to Fleischer (1991), awaruite refers to alloys in the compositional range Ni_2Fe to Ni_3Fe , but Nickel and Nichols (1991) listed awaruite as being generally accepted by the mineralogical community as Ni_3Fe . This is consistent with the X-ray powder pattern of awaruite in asbestos-bearing rocks from Quebec, Canada, that corresponds to that of artificial Ni_3Fe (Nickel, 1959). Danon et al. (1981) identified awaruite as Ni_3Fe in the Parambu chondrite by its Ni content, lattice parameter, and Mössbauer spectroscopic characteristics. Awaruite has occasionally been called “Ni-rich taenite,” but this term should be avoided because it has also been used to refer to tetrataenite (NiFe).

Since its discovery in New Zealand in 1885 (Ulrich, 1890), awaruite has been found in about 20 terrestrial localities as an accessory phase associated with partially serpentinized peridotite. Typical grain sizes are 10–300 μm , but rare grains as large as 4 mm have been found in the Sakhakot-Qila Complex in Pakistan (Ahmed and Bevan, 1981). Grain shapes typically are irregular, anhedral, or skeletal; in Poschiavo, Switzerland, awaruite occurs as a replacement mineral that is pseudomorphic after anhedral magnetite and pentlandite (de Quervain, 1945). There is no reported occurrence of euhedral awaruite or any evidence of zoning (Krishnarao, 1964). It is probable that all known occurrences of terrestrial awaruite formed at temperatures $\leq 750^\circ\text{C}$ during processes associated with the serpentinization of peridotite (Ramdohr, 1950; Nickel, 1959; Krishnarao, 1964; Frost, 1985).

Awaruite also occurs in several highly oxidized chondritic meteorites (e.g., Clarke et al., 1970). Minor occurrences of awaruite include (1) several LL3 ordinary chondrites wherein small anhedral grains occur in association with sulfides (pentlandite and troilite) and carbides {cohenite $[(\text{Fe},\text{Ni})_3\text{C}]$ and haxonite $[(\text{Fe},\text{Ni})_{23}\text{C}_6]$ } (Taylor et al., 1981); (2) LL5 Parambu wherein anhedral grains from 10 to 20 μm are associated with pentlandite, troilite, and a new metallic Fe phase with high Co and low Ni (Danon et al., 1981; Rubin, 1990); and (3) the highly oxidized chondrite ALH85151 wherein awaruite occurs both as isolated grains and as grains associated with pentlandite, troilite, and the new metallic Fe phase mentioned above (Rubin and Kallemeyn, 1989).

The most conspicuous occurrence of awaruite in meteorites is as subangular grains associated with magnetite, pentlandite, and troilite in opaque nodules inside porphyritic chondrules in oxidized CV3 carbonaceous chondrites such as Allende (Haggerty and McMahon, 1979; McMahon and Haggerty, 1980). The Ningqiang CK3-an chondrite (Kallemeyn et al., 1991) contains 0.5 vol% awaruite in opaque assemblages similar to those in Allende (Rubin et al., 1988). Haggerty and McMahon (1979) examined >1000 Allende chondrules in thin section; in

every awaruite-bearing opaque nodule in their study, the awaruite morphology was subangular to rounded; no euhedral grains were encountered (S. E. Haggerty, personal communication, 1990). Haggerty and McMahon (1979) suggested that subsolidus oxidation of low-Ni metal led to the formation of magnetite and (because Fe is oxidized more readily than Ni) Ni-rich metal (including tetraetaenite and awaruite).

Here I report the first known occurrence of zoned, euhedral awaruite. Several such grains occur in association with magnetite and pentlandite in an opaque nodule in an Allende chondrule. The occurrence of euhedral awaruite grains, which are likely to have formed from a melt, indicates that models invoking a solid-state origin of awaruite in CV chondrites need to be reevaluated.

ANALYTICAL PROCEDURES

For the purposes of an unrelated investigation, ~30 chondrules were separated from the Allende whole rock using stainless steel dental tools. The chondrules were individually cast in Castolite resin and polished on a cloth lap using diamond paste and ethanol lubricant until the tops of the chondrules were planed to depths of 15–20% of the chondrule radii. During reflected-light microscopic examination of the chondrules, a large opaque nodule with euhedral awaruite was discovered in one of them.

Olivine, pyroxene, and magnetite compositions were determined with the UCLA automated ARL-EMX electron microprobe using crystal spectrometers, natural and synthetic standards, counting times of 20 s, standard correction procedures (Bence and Albee, 1968), and a sample current of 15 nA at 15 kV. Awaruite and pentlandite compositions were determined with the UCLA automated Cameca Camebax electron microprobe using crystal spectrometers, counting times of 20 s, ZAF corrections, and a sample current of ~12 nA at 20 kV. The standards were pure Fe metal, pure Ni metal, NBS steel 1156 for Co (7.3 wt%), and Canyon Diablo troilite for S (36.5 wt%). Co background was obtained at wavelengths of 177.4 and 180.8 pm; these wavelengths were found to be the best suited for the elimination of the contribution of the $FeK\beta$ peak to the $CoK\alpha$ peak. Merrillite was analyzed with the Cameca probe at 15 kV using the following standards: fluorapatite for Ca and P, forsterite for Mg, and magnetite for Fe. Phases in the chondrule mesostasis were identified with the EDS of the Cameca probe. The possibilities of systematic errors in each probe were reduced by alternating analyses of magnetite, pentlandite, and awaruite in nodule 1 with analyses of these phases in other nodules in the chondrule as well as nodules in other Allende chondrules.

RESULTS

Petrography

Chondrule 90-1 (Fig. 1) is an ellipsoidal object measuring 1.9×2.4 mm separated from Allende. Based on

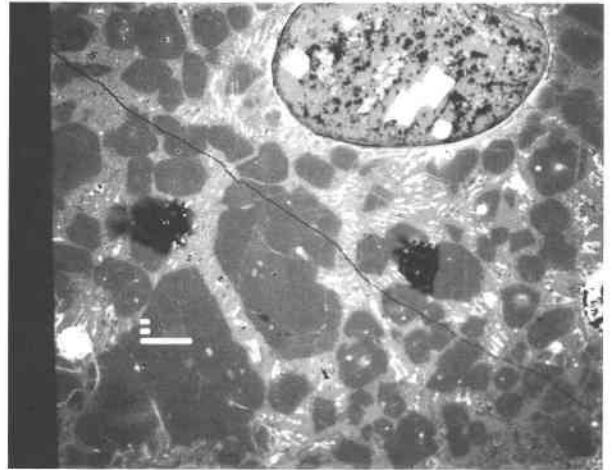


Fig. 1. Mosaic image of nodule 1 (reflected light) and surrounding chondrule (backscattered electrons); the euhedral, subhedral, and angular olivine phenocrysts (dark gray) of chondrule 90-1 are surrounded by an anorthitic mesostasis (medium gray) containing numerous pentlandite and magnetite grains (white). A crack (black line) traverses the chondrule from upper left to lower right. Nodule 1 (upper right) contains euhedral awaruite (white), blebby pentlandite (light gray), and abundant magnetite (medium gray). Dark areas in the chondrule and nodule are plucked regions. The long white bar at lower left is 100 μ m long.

the classification schemes for chondrule textural types developed by McSween (1977a), Gooding and Keil (1981), and Scott and Taylor (1983), the chondrule is a low-FeO (type IA) porphyritic olivine type. The chondrule consists mainly of 50–300 μ m euhedral, subhedral, and angular olivine phenocrysts (Fig. 1) ranging in composition from $Fa_{1.1}$ to $Fa_{8.2}$ (mean, 3.7 ± 1.9) and surrounded by a devitrified anorthitic mesostasis. (All Fa and Fs values are in mole percent.) Each of the phenocrysts is normally zoned in FeO; one representative grain ranges in composition from $Fa_{0.73}$ at the center to $Fa_{5.5}$ at the edge. At the inside edge of the chondrule are several grains of low-Ca pyroxene. These grains range in composition from $Fs_{1.2}$ to $Fs_{3.9}$ and average $Fs_{2.2 \pm 1.0}$. Like the olivine phenocrysts, each of the pyroxene grains is normally zoned in FeO; one typical grain ranges in composition from $Fs_{0.91}$ at the center to $Fs_{2.8}$ at the edge. At the edge of the chondrule is a relatively ferroan olivine grain ($Fa_{2.3}$) that was excluded from the mean olivine composition given above; this grain was probably derived from adhering matrix material rather than from the chondrule itself.

There are ten spheroidal to ellipsoidal magnetite-bearing nodules in the chondrule that range from 5 to 290×510 μ m (mean = 75 μ m) in apparent diameter. Some consist entirely of magnetite; others also contain awaruite \pm pentlandite \pm troilite (Fig. 2). Most contain accessory amounts of merrillite. Except in the largest nodule (described below), each awaruite grain has the rounded or subangular morphology typical for Allende opaque nodules (e.g., Fig. 1 of Haggerty and McMahon, 1979). In

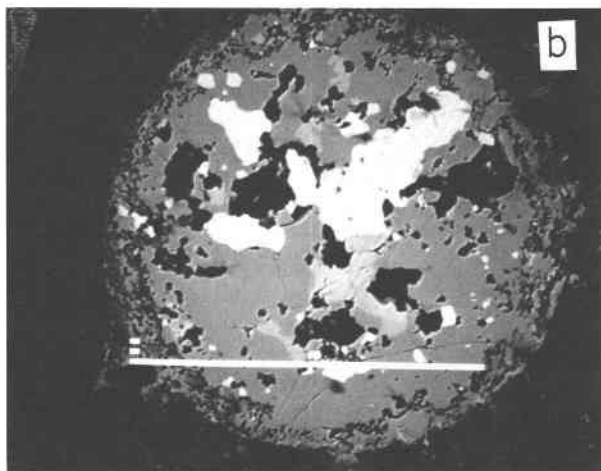
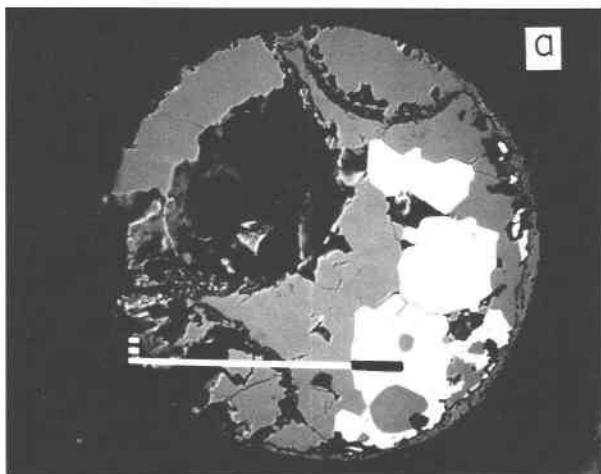


Fig. 2. Backscattered electron images of two additional opaque nodules in chondrule 90-1. Rounded to anhedral awaruite grains (white in a and b) are surrounded by magnetite (dark gray). The nodule in (b) contains some pentlandite (medium gray). Black areas are plucked regions. In both images, the scale bar is 100 μm long; in (a), the portion of the scale bar overlapping an awaruite grain is black.

addition to the magnetite-bearing nodules, there are a few nodules from 1 to 30 μm and isolated patches consisting principally of sulfide (pentlandite \pm troilite); some contain a few small, rounded awaruite grains. A few angular 5–10 μm magnetite and sulfide grains also occur in the chondrule mesostasis (Fig. 1). Altogether, opaque phases constitute ~ 5 vol% of chondrule 90-1.

The largest nodule (nodule 1) is $290 \times 510 \mu\text{m}$ in apparent size (Fig. 3); this is larger than any of the nodules examined by Haggerty and McMahon (1979) (< 5 – $250 \mu\text{m}$). Nodule 1 consists of 5 vol% pentlandite (occurring as 2–10 μm grains and $\leq 100 \mu\text{m}$ irregular blebby masses), 9 vol% euhedral awaruite crystals, 1 vol% merrillite (occurring as an irregular ring 1–5 μm thick near the margin of the nodule) and 85 vol% massive magnetite. Troi-

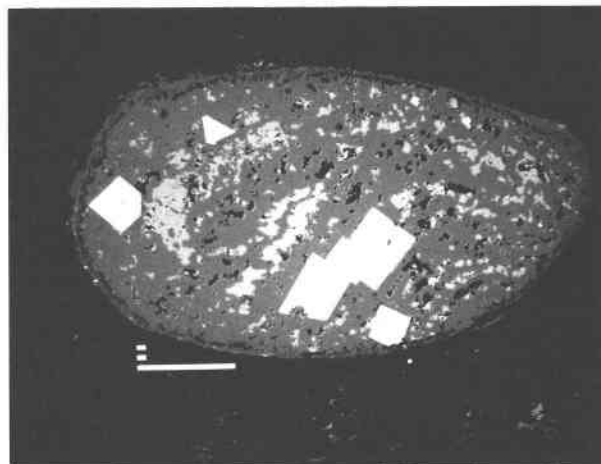


Fig. 3. Backscattered electron image of nodule 1. Euhedral awaruite (white) and blebby pentlandite (light gray) are surrounded by massive magnetite (dark gray). At the inside margin of the nodule, merrillite (black) forms an irregular ring around the entire nodule. Black regions outside the nodule are the silicate portions of the chondrule. The long white bar at lower left is 100 μm long.

lite is absent. There are six relatively large (35–65 μm) awaruite grains visible in nodule 1: two are nearly perfect cubes (square morphologies in plane), one is half of a cube (triangular morphology in plane), and three grains are grown together (two rectangles and one trapezoid in plane). In addition, two small (6–8 μm) grains occur near the nodule margin: one appears in plane view to be an intergrowth of a triangle and a trapezoid; the other, a trapezoid, is adjacent to pentlandite. There are no anhedral or rounded awaruite grains in the nodule.

Mineral chemistry and bulk composition

Magnetite in nodule 1 contains minor concentrations of Cr_2O_3 and accessory concentrations of MgO , NiO , and CaO (Table 1). Magnetite in other nodules in chondrule 90-1 and in other Allende chondrules contains significantly more Al_2O_3 (0.61 ± 0.14 vs. < 0.04 wt%) and marginally more CaO (0.10 ± 0.07 vs. 0.05 wt%).

Pentlandite in nodule 1 averages 28.4 ± 0.7 wt% Ni and 2.5 ± 0.3 wt% Co (Table 2); pentlandite in other nodules in chondrule 90-1 and in other Allende chondrules contains less Ni (19–21 wt%) and less Co (0.76–0.92 wt%).

The euhedral awaruite in nodule 1 averages 71.2 ± 0.4 wt% Ni and 2.1 ± 0.1 wt% Co (Table 2). The grains are zoned in Co: grain edges average only 1.9 wt% Co, whereas grain centers average 2.2 wt% Co; thus, there is an $\sim 15\%$ relative depletion of Co at grain edges. Anhedral or rounded awaruite in other nodules in chondrule 90-1 and in other Allende chondrules contains less Ni (65–67 wt%) but comparable amounts of Co (1.7–2.6 wt%). Co depletions at the edges of these other awaruite grains range from 0 to 5% compared to grain centers.

TABLE 1. Mean compositions (wt%) of magnetite in Allende opaque nodules

	90-1	90-1	90-1	90-1	90-2
Chondrule	90-1	90-1	90-1	90-1	90-2
Nodule	1	2	3	4	6
No. of points	9	2	2	1	1
SiO ₂	<0.04	0.06	0.05	0.07	0.06
TiO ₂	<0.04	<0.04	<0.04	<0.04	<0.04
Al ₂ O ₃	<0.04	0.74	0.54	0.72	0.45
Cr ₂ O ₃	1.1 ± 0.2	1.4	0.85	0.71	1.1
FeO*	91.6 ± 1.0	91.3	90.7	91.4	91.2
MnO	<0.04	<0.04	0.06	<0.04	<0.04
NiO	0.13 ± 0.08	0.22	0.19	0.08	0.37
MgO	0.22 ± 0.05	0.07	0.11	0.14	0.50
CaO	0.05 ± 0.05	0.04	0.15	0.17	<0.04
Total**	93.1	93.8	92.6	93.3	93.7

* All Fe is given as FeO.

** An additional 6.8 wt% O should be added to the totals of all of the nodules except nodule 3 (6.7 wt% O).

Although no troilite occurs in nodule 1, a few grains occur in other nodules in chondrule 90-1 as well as in the chondrule mesostasis. These grains are essentially stoichiometric FeS with low concentrations of Ni (<0.06–0.15 wt%) and no detectable Co.

Merrillite in nodule 1 contains significant amounts of MgO and FeO (Table 3).

The bulk composition of nodule 1 (Table 4) was determined from modal mineral abundances, mineral compositions, and the following estimated specific gravities: magnetite, 5.2; awaruite, 8.4; merrillite, 3.1; and pentlandite, 4.7. Other nodules contain more Al and have higher bulk Fe/Ni ratios.

DISCUSSION

Chondrule formation

Chondrule 90-1 has a typical texture for a low-FeO porphyritic olivine chondrule; it has igneously zoned olivine and low-Ca pyroxene phenocrysts and a devitrified feldspathic mesostasis (Fig. 1). The chondrule formed from a melt, almost certainly by the flash heating and incomplete melting of a preexisting solid precursor in the solar nebula (e.g., Grossman, 1988). Surface tension

TABLE 2. Mean compositions (wt%) of awaruite and pentlandite in Allende opaque nodules

	Awaruite					
Chondrule	90-1	90-1	90-1	90-1	90-1	90-2
Nodule	1	2	3	4	5	6
No. of points	23	3	2	3	1	2
Fe	27.3 ± 0.5	32.8	30.1	32.2	32.5	31.3
Co	2.1 ± 0.1	2.1	1.7	2.6	2.4	2.1
Ni	71.2 ± 0.4	65.7	67.5	65.7	65.3	67.3
Total	100.6	100.6	99.3	100.5	100.2	100.7
	Pentlandite					
Chondrule	90-1	90-1				90-2
Nodule	1	2				6
No. of points	6	2				4
Fe	37.0 ± 0.9	46.6				45.1
Co	2.5 ± 0.3	0.76				0.92
Ni	28.4 ± 0.7	19.2				20.6
S	32.9 ± 0.6	33.6				33.4
Total	100.8	100.2				100.0

TABLE 3. Composition (wt%) of merrillite in nodule 1

No. of points	1
FeO	3.7
MgO	3.2
CaO	46.1
P ₂ O ₅	46.3
Total	99.3

caused the partly molten droplet to assume its ellipsoidal shape. Existing experimental data (Hewins, 1988) indicate that temperatures may have reached ~1600 °C during the heating event and that afterwards the droplet cooled at 100–1000 °C h⁻¹.

Opaque nodule formation

As pointed out by Haggerty and McMahon (1979), the sulfide-rich nodules in Allende structurally and texturally resemble sulfide ± oxide spherules that formed as immiscible liquids within terrestrial basalts (e.g., Desborough et al., 1968; Moore and Calk, 1971).

The magnetite-rich nodules in Allende are analogous to the kamacite blebs that occur commonly in low-FeO (type I) porphyritic chondrules in ordinary, CO, and reduced CV chondrites; these kamacite blebs formed from melt globules of metal ± sulfide that were immiscible in the surrounding silicate liquid of the chondrule. The spheroidal to ellipsoidal shapes of the magnetite-rich nodules indicate that they or their precursors must have formed from melt droplets that were immiscible with the surrounding silicate mush.

Haggerty and McMahon (1979) suggested that the magnetite-rich nodules formed by subsolidus oxidation of preexisting kamacite-rich nodules. During the oxidation event, much of the hypothesized kamacite was transformed into magnetite; because Fe is oxidized more readily than Ni, the residual metal became increasingly rich in Ni and formed tetrataenite and awaruite. There are a number of potential problems with this scenario including the unknown source of the oxidation, the lack of petrographic evidence for the large (factor of 2) change in molar volume expected when kamacite changes into magnetite, and the juxtaposition in Allende of metal-free chondrules containing magnetite with magnetite-free chondrules containing metal (McSween, 1977b). Further-

TABLE 4. Bulk composition (wt%) of nodule 1*

O	22.7
Mg	0.1
P	0.1
S	1.4
Ca	0.2
Cr	0.6
Fe	63.4
Co	0.4
Ni	11.1
Total	100.0

* Determined from modal abundances, mineral compositions, and estimated densities (see text).

more, subsolidus oxidation reactions are unlikely to create euhedral awaruite grains such as those in nodule 1 unless the awaruite is pseudomorphic after a preexisting euhedral cubic phase (cf. Krishnarao, 1964); however, in petrographic examination of thin sections of three reduced CV chondrites (Efremovka, Leoville, and Vigarno), I found no occurrences of euhedral cubic minerals associated with kamacite.

Even if awaruite grains with euhedral morphologies could somehow have been produced by subsolidus oxidation, it seems unlikely that they would have developed an ~15% relative depletion of Co at their edges. Although this depletion could possibly have resulted from postagglomeration reduction, such a process would have equally affected other awaruite grains throughout Allende; instead the maximum depletion of Co in these grains is much less than (only ~30% of) those in the euhedral grains.

In view of these objections, it seems unlikely that the magnetite- and awaruite-bearing nodules in Allende formed by subsolidus oxidation of kamacite. Other mechanisms should be considered.

McMahon and Haggerty (1980) discussed an alternative, i.e., that sulfide, magnetite, and Ni-rich metal precipitated directly from a chondrule melt. An increase in the f_{O_2} of the melt could have resulted in the formation of Fe^{3+} from FeO and metallic Fe, leading to the crystallization of magnetite; this would have decreased FeO in the residual silicate liquid and caused the liquid to become saturated in S. As the chondrule cooled, independent sulfide globules and complexes of sulfide + magnetite + metallic Fe-Ni could have formed. The major objection to this model is the difficulty of significantly increasing the f_{O_2} of the chondrule melt to allow magnetite crystallization from chondrules that had little or no Fe^{3+} initially; the difficulty is compounded by the requirement of the model that this process occurred in the majority of porphyritic chondrules in Allende (most of which now possess opaque nodules). Furthermore, if the f_{O_2} commonly increased sufficiently to cause magnetite to crystallize, then in some porphyritic chondrules it should have been high enough to cause Ni to oxidize and enter the olivine; however, NiO concentrations in Allende chondrule olivines are very low (Simon and Haggerty, 1979).

A more plausible alternative is that kamacite within the solid precursors of Allende chondrules was oxidized in the nebula and transformed into magnetite when temperatures cooled below ~130 °C (e.g., Larimer, 1988). Residual metal became rich in Ni. Some of the kamacite may have previously experienced sulfidation at higher nebular temperatures. The present magnetite-rich assemblages could have acquired their rounded shapes during the brief period of chondrule formation, provided they were immiscible with the surrounding silicate mush.

Nebular oxidation is supported by Hua et al. (1988) who described fayalite-rich halos around small metallic Fe-Ni inclusions inside olivine grains in CV3 chondrites.

They interpreted this assemblage as having formed in the nebula by in situ oxidation of the metallic Fe-Ni followed by diffusion of FeO into the surrounding forsterite. A by-product of such a process would be an increase in the Ni concentration of the residual metal.

Formation of euhedral awaruite

Nodule 1 differs from other opaque nodules in its larger size (290 × 510 vs. <5–250 μm), euhedral morphology of constituent awaruites, and bulk composition that is lower in Al_2O_3 and has a somewhat higher Ni/Fe ratio. These distinctive characteristics indicate that nodule 1 did not form in exactly the same manner as the other opaque nodules. Nevertheless, its close mineralogical resemblance to the other nodules indicates that all nodules must have formed by the same general process.

The most straightforward manner in which euhedral crystals form is by primary crystallization from a melt. I assume here that nodule 1 formed from a melt with approximately the same composition as the present nodule (Table 4) and that the melt was immiscible with the surrounding silicate mush during chondrule formation. The liquidus relations for a melt with approximately this composition can be plotted on the Fe-S-O diagram of Naldrett (1969) by adding Ni and Co to Fe and assuming that the diagram will not be significantly changed (Fig. 4). This assumption is reasonable: Craig and Naldrett (1967) found that for concentrations of up to 20 wt% Ni substituting for Fe, melting temperatures are not lowered measurably below those determined for the Fe-S-O system. In the adapted liquidus diagram for this system (Fig. 4), nodule 1 plots within the narrow band of the metallic Fe-Ni field, between the two-liquid and wüstite fields. These relations indicate that metallic Fe-Ni was the first phase to crystallize from the nodule melt, probably at a temperature of ~1400 °C (Naldrett, 1969). At such a high temperature, the metallic Fe-Ni phase is taenite (fcc), irrespective of Ni concentration. The large difference in surface energy between the crystallizing taenite and the surrounding magnetite-rich liquid helped ensure the development of euhedral morphologies in the taenite grains.

Of the three metallic Fe-Ni grains that grew together (Fig. 3), one (at top) contains a small inclusion of magnetite and one (at bottom) appears to impinge on a magnetite grain. This suggests either that during chondrule formation not all of the magnetite was melted or that some magnetite cocrystallized with taenite as the nodule cooled.

For nonmetallic liquids, it is probable that Co has a solid-liquid distribution coefficient (K_d) > 1 (J. T. Wasson, personal communication, 1990). Thus, the first taenite crystals to form acquired more Co than subsequently crystallizing taenite. The ~15% relative depletion in Co at awaruite grain edges compared to grain centers may have resulted from such igneous zoning. Eventually, magnetite, sulfide, and phosphate also crystallized. The merillite ring at the edge of the nodule suggests that it was essentially the last phase to crystallize from the immis-

cible melt droplet; only small amounts of magnetite crystallized afterwards, outside the merrillite ring.

The minor differences in composition between nodule 1 and the other magnetite-bearing nodules in chondrule 90-1 may have been sufficient to change the liquidus relations so that taenite was not the first phase to crystallize in the other nodules. Although they also crystallized directly from magnetite-rich melts, metallic Fe-Ni grains with euhedral morphologies did not form in them. The slightly deviant composition of nodule 1 (i.e., low Al_2O_3 ; high Ni/Fe ratio) may have been inherited from heterogeneities in the chondrule precursor.

As the nodule cooled below $\sim 500^\circ\text{C}$, the euhedral taenite grains, having ~ 71 wt% Ni, may have transformed directly into awaruite of the same composition (Fig. 15 of Reuter et al., 1988). Other nodules possessing taenite with lower Ni concentrations (65–67 wt%) entered the tetraetaenite-awaruite two-phase region and precipitated both phases (Reuter et al., 1988).

The major problem with this model is the unproven assumption that liquids as rich in FeO as the magnetite-rich opaque nodules would be immiscible in a silicate melt under the peculiar conditions of chondrule formation. However, this assumption is amenable to testing.

In an alternative model, the euhedral awaruite grains in nodule 1 are considered to be idiomorphs, analogous to crystals commonly found in terrestrial metamorphic rocks (e.g., garnet in micaceous schist; diopside in marble). It is possible that during thermal metamorphism of Allende (McSween, 1977b), the awaruite grains in nodule 1 developed idiomorphic morphologies, in part because of the large difference in surface energy between the awaruite and surrounding magnetite. There are three objections to this model: (1) Allende is still a type-3 chondrite and probably has not been heated much above 600°C (Dodd, 1981); (2) the other awaruite grains in chondrule 90-1 (as well as those in thousands of nodules in other Allende chondrules) are also surrounded by magnetite but do not exhibit idiomorphic morphologies; and (3) the few metamorphosed ordinary chondrites that are highly oxidized (e.g., LL5 Parambu) contain anhedral but not idiomorphic awaruite (Rubin, 1990).

SUMMARY

It seems likely that all the awaruite grains in Allende porphyritic chondrules formed by the following mechanism: (1) nebular oxidation of kamacite in chondrule precursor dustballs, (2) chondrule formation during an episode of flash melting, (3) development of immiscible magnetite-rich melt droplets within the surrounding silicate mush, (4) crystallization of taenite and magnetite (plus or minus sulfide and phosphate) in the droplets to form opaque nodules, and (5) cooling of the nodules to $\leq 500^\circ\text{C}$ and transformation of taenite into awaruite \pm tetraetaenite. The formation of the euhedral awaruite grains in nodule 1 differs from that of anhedral grains in other nodules only in the order in which awaruite and magnetite crystallized: awaruite was the sole liquidus phase in

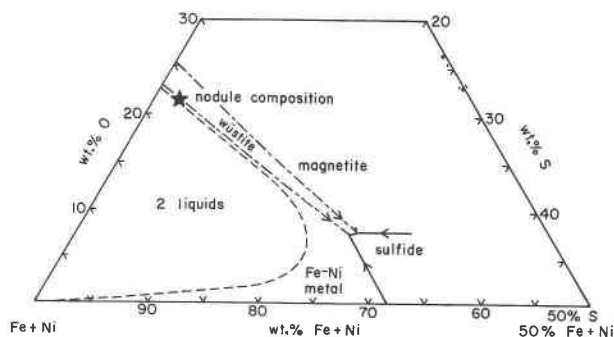


Fig. 4. A portion of the Fe-Ni-S-O phase diagram for low concentrations of Ni (adapted from Naldrett, 1969). The bulk composition of euhedral-awaruite-bearing nodule 1 (star symbol) plots inside the narrow band of the metallic Fe-Ni field between the two-liquid and wüstite fields, indicating that metallic Fe-Ni (taenite) was the liquidus phase. Other opaque nodules differ somewhat in composition and probably did not have metallic Fe-Ni as their sole liquidus phase.

nodule 1 but crystallized along with or subsequent to magnetite in the other nodules.

ACKNOWLEDGMENTS

I thank the following people for helpful discussion: J.T. Wasson, G.J. Taylor, J.N. Grossman, E.J. Olsen, J.I. Goldstein, A. Montana, W.A. Dollase, E.A. Jerde, J. Jones, and S.S. Sorensen. Technical assistance was provided by T. Jen, J. Ma, S. Tir, and R.E. Jones. The paper benefited from reviews by J.I. Goldstein and E.R.D. Scott and comments by W.D. Carlson. This work was supported in part by NASA grant NAG 9-40.

REFERENCES CITED

- Ahmed, Z., and Bevan, J.C. (1981) Awaruite, iridian awaruite, and a new Ru-Os-Ir-Ni-Fe alloy from the Sakhakot-Qila Complex, Malakand Agency, Pakistan. *Mineralogical Magazine*, 44, 225–230.
- Bence, A.E., and Albee, A.L. (1968) Empirical correction factors for the electron microanalysis of silicates and oxides. *Journal of Geology*, 76, 382–403.
- Clarke, R.S., Jarosewich, E., Mason, B., Nelen, J., Gomez, M., and Hyde, J.R. (1970) The Allende, Mexico, meteorite shower. *Smithsonian Contributions to the Earth Sciences*, 5, 1–53.
- Craig, J.R., and Naldrett, A.J. (1967) Minimum melting of nickeliferous pyrrhotite ores. *Carnegie Institution of Washington Year Book*, 66, 417–419.
- Danon, J., Christophe Michel-Lévy, M., Jehanno, C., Keil, K., Gomes, C.B., Scorzelli, R.B., and Souza Azevedo, I. (1981) Awaruite (Ni_3Fe) in the geminitic LL chondrite Parambu. Formation under high $f\text{O}_2$ (abs.). *Meteoritics*, 16, 305.
- de Quervain, F. (1945) Awaruit und Pentlandit im Serpentin von Selva bei Poschiavo. *Schweizerische Mineralogische und Petrographische Mitteilungen*, 25, 305–311.
- Desborough, G.A., Anderson, A.T., and Wright, T.L. (1968) Mineralogy of sulfides from certain Hawaiian basalts. *Economic Geology*, 63, 636–644.
- Dodd, R.T. (1981) *Meteorites—a petrologic-chemical synthesis*, 368 p. Cambridge University Press, New York.
- Fleischer, M. (1991) *Glossary of mineral species* (6th edition), 256 p. Mineralogical Record, Inc., Tucson, Arizona.
- Frost, B.R. (1985) On the stability of sulfides, oxides, and native metals in serpentinite. *Journal of Petrology*, 26, 31–63.
- Gooding, J.L., and Keil, K. (1981) Relative abundances of chondrule primary textural types in ordinary chondrites and their bearing on conditions of chondrule formation. *Meteoritics*, 16, 17–43.

- Grossman, J.N. (1988) Formation of chondrules. In J.F. Kerridge and M.S. Matthews, Eds., *Meteorites and the early solar system*, p. 680–696. University of Arizona Press, Tucson, Arizona.
- Haggerty, S.E., and McMahon, B.M. (1979) Magnetite-sulfide-metal complexes in the Allende meteorite. *Proceedings of the Tenth Lunar and Planetary Science Conference. Geochimica et Cosmochimica Acta*, 11, 851–870.
- Hewins, R.H. (1988) Experimental studies of chondrules. In J.F. Kerridge and M.S. Matthews, Eds., *Meteorites and the early solar system*, p. 660–679. University of Arizona Press, Tucson, Arizona.
- Hua, X., Adam, J., Palme, H., and El Goresy, A. (1988) Fayalite-rich rims, veins, and halos around and in forsteritic olivines in CAIs and chondrules in carbonaceous chondrites: Types, compositional profiles and constraints of their formation. *Geochimica et Cosmochimica Acta*, 52, 1389–1408.
- Kallemeyn, G.W., Rubin, A.E., and Wasson, J.T. (1991) The compositional classification of chondrites: V. The Karoonda (CK) group of carbonaceous chondrites. *Geochimica et Cosmochimica Acta*, 55, 881–892.
- Krishnarao, J.S.R. (1964) Native nickel-iron alloy, its mode of occurrence, distribution and origin. *Economic Geology*, 59, 443–448.
- Larimer, J.W. (1988) The cosmochemical classification of the elements. In J.F. Kerridge and M.S. Matthews, Eds., *Meteorites and the early solar system*, p. 375–389. University of Arizona Press, Tucson, Arizona.
- Leech, P., and Sykes, C. (1939) The evidence for a superlattice in the nickel-iron alloy Ni₃Fe. *Philosophical Magazine Journal of Science*, 27, 742–753.
- McMahon, B.M., and Haggerty, S.E. (1980) Experimental studies bearing on the magnetite-alloy-sulfide association in the Allende meteorite: Constraints on the conditions of chondrule formation. *Proceedings of the 11th Lunar and Planetary Science Conference. Geochimica et Cosmochimica Acta*, 14, 1003–1025.
- McSween, H.Y. (1977a) Chemical and petrographic constraints on the origin of chondrules and inclusions in carbonaceous chondrites. *Geochimica et Cosmochimica Acta*, 41, 1843–1860.
- (1977b) Petrographic variations among carbonaceous chondrites of the Vigarano type. *Geochimica et Cosmochimica Acta*, 41, 1777–1790.
- Moore, J.G., and Calk, L. (1971) Sulfide spherules in vesicles of dredged pillow basalt. *American Mineralogist*, 56, 476–488.
- Naldrett, A.J. (1969) A portion of the system Fe-S-O between 900 and 1080 °C and its application to sulfide ore magmas. *Journal of Petrology*, 10, 171–201.
- Nickel, E.H. (1959) The occurrence of native nickel-iron in the serpentine rock of the eastern townships of Quebec province. *Canadian Mineralogist*, 6, 307–319.
- Nickel, E.H., and Nichols, M.C. (1991) *Mineral reference manual*, 250 p. Van Nostrand Reinhold, New York.
- Ramdohr, P. (1950) Über Josephinit, Awaruit, Souesit, ihre Eigenschaften, Entstehung und Paragenesis. *Mineralogical Magazine*, 29, 374–394.
- Reuter, K.B., Williams, D.B., and Goldstein, J.I. (1988) Low temperature phase transformations in the metallic phases of iron and stony-iron meteorites. *Geochimica et Cosmochimica Acta*, 52, 617–626.
- Rubin, A.E. (1990) Kamacite and olivine in ordinary chondrites: Inter-group and intragroup relationships. *Geochimica et Cosmochimica Acta*, 54, 1217–1232.
- Rubin, A.E., and Kallemeyn, G.W. (1989) Carlisle Lakes and Allan Hills 85151: Members of a new chondrite grouplet. *Geochimica et Cosmochimica Acta*, 53, 3035–3044.
- Rubin, A.E., Wang, D., Kallemeyn, G.W., and Wasson, J.T. (1988) The Ningqiang meteorite: Classification and petrology of an anomalous CV chondrite. *Meteoritics*, 23, 13–23.
- Scott, E.R.D., and Taylor, G.J. (1983) Chondrules and other components in C, O, and E chondrites: Similarities in their properties and origins. *Proceedings of the 14th Lunar and Planetary Science Conference. Journal of Geophysical Research*, 88, B275–B286.
- Simon, S.B., and Haggerty, S.E. (1979) Petrography and olivine mineral chemistry of chondrules and inclusions in the Allende meteorite. *Proceedings of the 11th Lunar and Planetary Science Conference. Geochimica et Cosmochimica Acta*, 14, 871–883.
- Taylor, G.J., Okada, A., Scott, E.R.D., Rubin, A.E., Huss, G.R., and Keil, K. (1981) The occurrence and implications of carbide-magnetite assemblages in unequilibrated ordinary chondrites (abs.). *Lunar and Planetary Science*, 12, 1076–1078.
- Ulrich, G.H.F. (1890) On the discovery, mode of occurrence, and distribution of the nickel-iron alloy awaruite, on the west coast of the South Island of New Zealand. *Quarterly Journal of the Geological Society of London*, 46, 619–633.

MANUSCRIPT RECEIVED JUNE 10, 1990

MANUSCRIPT ACCEPTED APRIL 15, 1991